2004 International Symposium on Nonlinear
Theory and its Applications (NOLTA2004)
Fukuoka, Japan, Nov. 29 - Dec. 3, 2004

Spatiotemporal Wave Dynamics and Power-law Scaling in Large Arrays of Fluid-elastic Oscillators with Applied Impact Constraint

Masaharu Kuroda[†], Ronald F. Clemens[‡], Francis C. Moon[‡]

†Applied Complexity Engineering Research Group, National Institute of Advanced Industrial Science and Technology
1-2-1 Namiki, Tsukuba, Ibaraki 305-8564, Japan
‡ Sibley School of Mechanical and Aerospace Engineering, Cornell University
204 Upson Hall, Ithaca, New York 14853-7501, USA
Email:m-kuroda@aist.go.jp, rfc6@cornell.edu, fcm3@cornell.edu

Abstract– We have performed experiments on spatiotemporal pattern formation in a large array of vertically cantilevered elastic rods arranged on a two-dimensional lattice in a uniform cross-flow. Simple experiments using an elastic-rod array were performed in a wind tunnel. Despite their simplicity, such experiments allow the observation of a variety of complex dynamical phenomena.

1. Introduction

"Self-organization" is considered to be as one of the key concepts which could become the basis of a new paradigm in a variety of engineering fields, ranging from generation of a new material at the nanometer level to the behavior of human groups at the macroscopic level. In order to bring about progress in these fields, it is important to first clarify the principle of self-organization as it is observed in nonlinear elements.

This research project aims at elucidating the basic mechanism of self-organization appearing in nonlinear systems with super-many degrees of-freedom, not only in the field of mechanical engineering, but also in interdisciplinary fields of science and technology. We decide to study the complex fluid-excited vibrations exhibited by an array of vertically-cantilevered elastic rods densely arranged on a lattice in a uniform cross-flow, as a model experiment. From the viewpoint of the realization of a large number of homogeneous oscillators, this experimental object consisting of many rods is considered to be suitable, as a model, for the verification of the principles involved, because this system cannot be further simplified in the field of mechanical engineering.

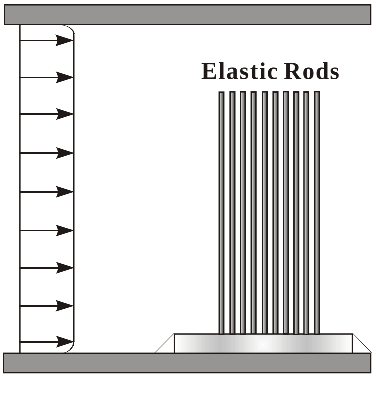

Fig. 1 Schematic diagram of the experimental setup

2. Experimental Setup and Conditions

Figure 1 shows a schematic diagram of our experimental setup. Rod-like structures were cantilevered at the base, and were free to vibrate at the tip in a wind tunnel. The interaction among the rods can be explained on the basis of two kinds of forces. One is the fluid force due to the wind disturbed by the motions of neighboring rods, and the other is the direct-impact force between the rods, when their vibration amplitude becomes too large.

In the experiment, various kinds of rod arrays were used. The first eigen-frequency of a steel rod used in the experiment is 26 Hz, while that of a polycarbonate rod used in the experiments is 18 Hz.

The wind tunnel was a low-turbulence system with a cross section of 25.6 cm x 25.6 cm. Wind speeds ranged from 0 to 12.0 m/s. The Reynolds number based on the rod diameter ranged from 200 to 900. Equipped with small accelerometer probes so that dynamic data could be obtained, a test rig was arranged inside the test section, and floodlights, which are necessary for recording the experiment 0n videotape, were located under the test section.

3. The Clustering of Vibrating Rods

We will discuss first the hierarchical spatiotemporal pattern observed in an array of 300 steel rods array (10 rows x 30 columns) subjected to a wind-tunnel experiment. The entire motion of the rod array was captured by a video camera located above the test section.

First of all, in the low wind-speed condition of around 3.5 m/s, fluid-elastic forces were found to govern the movement of the rods. The rods were free to move individually at this wind speed. Observed from the top, the rod tips did not show any significant dynamics in their distribution density over time.

Next, in the middle wind-speed condition of about 7.0 m/s, not only fluid-elastic forces but also direct impact between the rods started to affect the behavior of the rods. As for the distribution of rod density, the dense parts and the sparse parts alternated remarkably as time elapsed, and finally clusters, or collective movement of some of the rods, emerged. We confirmed that these clusters do not move according to a specific temporal pattern at this wind speed.

Finally, in the high wind-speed condition of approximately 10.5 m/s, the dominant force determining rod behavior shifted from fluid-elastic forces to direct impact. The most characteristic and important thing is that those clusters were linked together as in a chain, and that these chains were born at both corners on the front row; they moved coherently and repeatedly in the diagonal direction toward the backmost row as waves do. As an example, a series of contour maps of the distribution of rod density at high wind speed is shown in Figure 2.

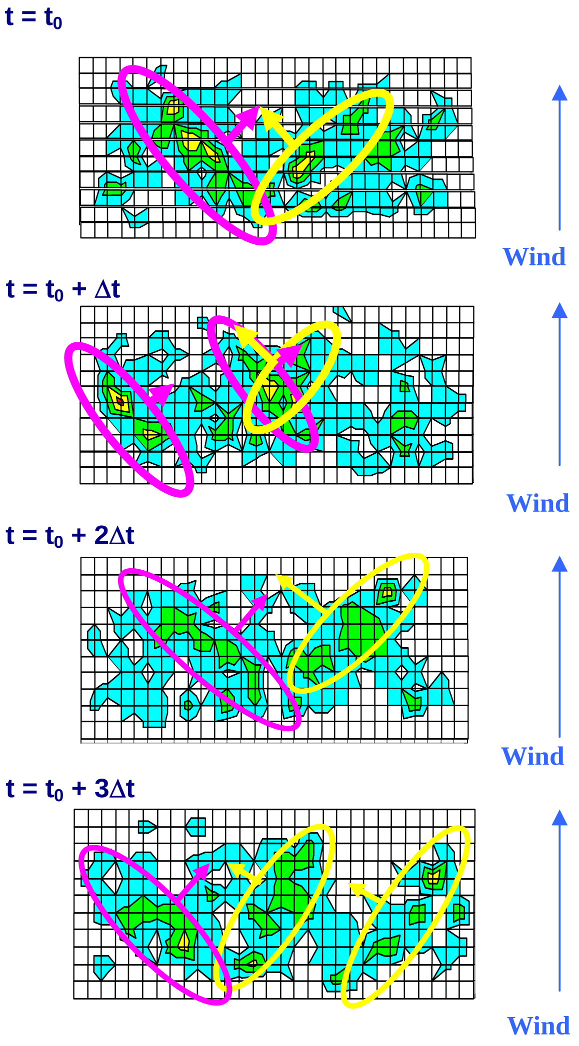

Fig. 2 A sequence of contour maps of the distribution of rod density at high wind speed (an array of 300 steel rods, Δt = 1/15 s)

4. The Power Law of the Spatiotemporal Pattern Formation

Secondly, we will discuss how the rate of the rod-to-rod collisions obtained experimentally can support the idea that the chain reaction of the sub-critical Hopf bifurcations may be a cause of global pattern generation.

Time-series data were obtained from a small accelerometer placed at a height of 1 cm from the base of the front-center rod. Figure 3 shows an example of the data at the wind speed of 11.2 m/s. The acceleration data suggested two kinds of motion, that is, recurrences of the bursting phenomena due to the rod-to-rod collisions over a long time scale (see Fig. 3a) and waveforms due to the impulse response of the rods over a short time scale (see Fig. 3b).

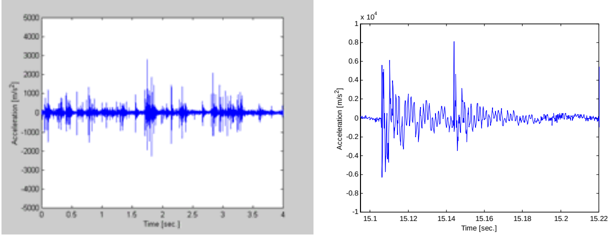

(a) (b) Magnification

Fig. 3 Acceleration at the front-center rod, at a wind speed of 11.2 m/s

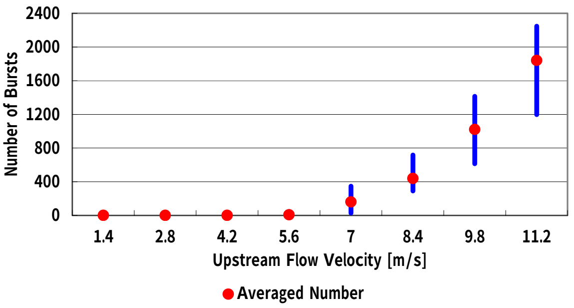

Threshold = 0.5 x 10^4 m/s^2

Fig. 4 Number of bursts between the rods as a function of wind speed

The time-series data for the acceleration observed across a 24-second interval were recorded, and the number of burst waveforms was automatically counted by a peak counter program based on the MATLAB® software. Setting the proper thresholds for the acceleration signals allowed us to distinguish a burst peak from a free vibration after a peak. Figure 4 shows a plot of the number of burst waveforms as a function of wind speed. On the graph, the bar and the solid circle represent the distribution range and the average number, respectively, for ten measurements at each wind speed.

As explained before, in the middle wind-speed condition, not only fluid-elastic forces but also direct impact between the rods started to affect rod behavior. Finally, in the high wind-speed condition, the dominant force determining rod behavior shifted from fluid-elastic forces to direct impact. This can be explained by the fact that the frequency of bursts at 10.5 m/s was ten times greater than that at 7.0 m/s, as shown in Figure 4. It was also mentioned before that, as the intensity of the interaction between neighboring rods increased, entire groups of rods achieved a better-organized behavior globally. We could easily guess that an increase in the rod-to-rod collision frequency would promote a change in the spatiotemporal pattern, as shown previously [1].

Therefore, we investigated whether the relationship between the increase in the rod-to-rod collision rate and the increase in flow speed can characterize this hierarchical pattern formation. We confirmed that scaling relationship is involved in the generation of clusters, that is, in the distribution of rod density. The basic relationship between the number of bursts and wind speed is expressed by the following equation:

$$V^2 = cN^\alpha \tag{1}$$

Here, V represents wind velocity, N shows the number of bursts and c is a constant. The term V^2 is proportional to the energy inputted into the rod array. By taking the logarithm of both sides of Eq. (1), we obtain a log N - log V plot. For example, we obtained the graph slope, and it indicates that α is almost 0.242 from Figure 4. In the final analysis, the results of ten experiments were used to obtain the graph slopes, and we were able to conclude that α is almost equal to 0.25. Therefore, the relationship between the energy inputted into the rod array by the air flow and the rate of rod collision complies with a power law with an exponent of 0.25.

In Davies and Moon's experimental research ([2]) into the spatiotemporal dynamics of a single row of Toda-type oscillators, the elastic oscillators connected by easily buckled elastic beams were excited by a periodic external force, and the motion of the oscillators made a transition from periodic dynamics to chaotic spatiotemporal waves as the external disturbance increased. In our research, the rod arrays were two-dimensional, and the disturbance, which was induced by turbulence due to the vortex shedding around the cylinders, had a strongly stochastic nature. In contrast with Davies and Moon's experiments, however, as the constraint, such as the collisions between rods, became more frequent with increased flow velocity, the behavior of the rod group developed dynamically from a small random-like movement to a global wave-like pattern which was coherent and well-organized.

5. The Generation of Wave Motion as a Global Spatiotemporal Pattern

The final topic concerns our experiments with an array of 1000 polycarbonate rods (40 rows x 25 columns), in which a wave-like motion was generated and intensified.

Even in the low wind-speed condition of around 4.20 m/s, we could see a variety of wave motions on the videotape recording of the experiments. For example, it is easy to confirm that a wave is propagating along each edge of the rod array. The spatial wavelengths of these waves are especially noticeable, because the wavelength is different depending on the wind velocity.

In the middle wind-speed condition of about 6.30 m/s, one can also see waves proceeding along the boundary

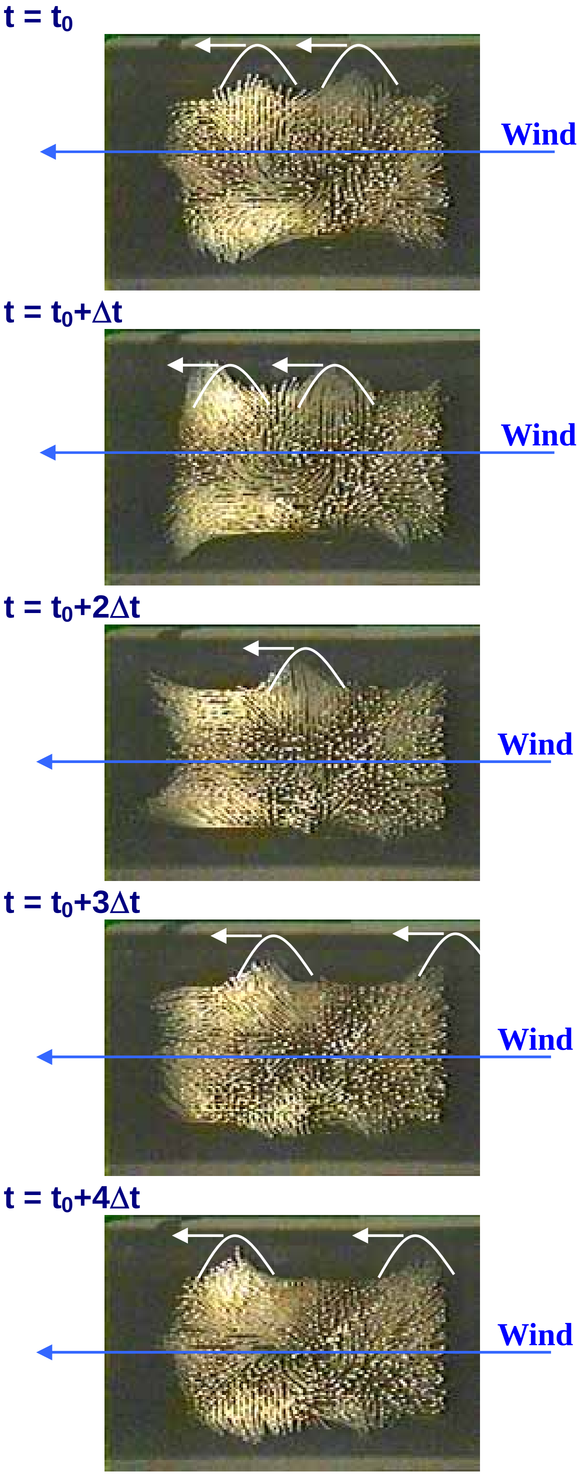

Fig. 5 A sequence of VTR frames at high wind speed ($\Delta T = 1/12$ s, top-view of the array of 1000 polycarbonate rods in a cross-flow of air)

edges of the array. In addition to those waves, one can see waves passing through the center of the array.

In the high wind-speed condition of approximately 8.40 m/s, one can still see waves proceeding along the boundary edges of the array. Figure 5 shows some successive VTR frames. The wave passing through the center of the array at high wind speed looks more complicated than that at middle wind speed.

The reason why emphasis is put on waves progressing along the longitudinal edges of the array is that their spatial wavelengths can be clearly measured from the videotaped images. The results are shown in Figure 6. Here, the length of the longitudinal edge of the rod array is 31.3 cm. The faster the upstream flow velocity, the longer the spatial wavelength of the wave traveling along the longitudinal edge of the rod array, although the graph slopes for the low, middle and high wind-speed conditions were different, depending on the air-flow speed in the wind tunnel.

By examining the acceleration signals, we found several characteristic wave frequencies exist. For example, Figure 7 shows the result of a cross-spectrum analysis using two accelerometer outputs. One is an acceleration signal from the front-left rod, and the other is that from the back-left rod. Higher-order vibration modes of the rod are excited by the direct impact between the rods. Below the first eigen-frequency of the rod, we can discern the presence of the characteristic wave frequency caused by the wave traveling along the left-side longitudinal edge of the rod array.

6. Conclusions

Nonstationary complex phenomena occurring in large arrays of up to 1000 vibrating rods in a wind tunnel were investigated in this experiment.

(1) There is a critical flow velocity at which a global dynamic pattern emerges in the entire rod array.

(2) A power law governs the scaling relationship between the rod impact rate and the flow velocity.

(3) A global spatiotemporal order emerges remaining local complexity as the flow speed increases.

(4) A wave motion can be observed along the edges of the array of 1000 polycarbonate rods.

Simple experiments using an elastic-rod array were performed in a wind tunnel. Despite their simplicity, such experiments allow the observation of a variety of complex spatiotemporal dynamics. In the study of complex systems, parameter changes commonly reveal novel relationships among elements. Such relationships emphasize the self-organization of hierarchical dynamic structures. It is noteworthy that the existence of such phenomena can also be confirmed in the field of mechanical engineering.

This research is directly applicable to nonlinear vibration problems which affect heat-exchanger pipes, pin-fin type heat sinks for personal computers, "honami" waves in rice fields, and the biomechanics of dowle. Moreover, the results of our experiments can also be applied in planning the position of planted trees to ensure wind protection, and in other projects in the fields of civil engineering, forestry, and agriculture. Our experiment object may also constitute a two-dimensional analog of flowing granular materials, at least from the viewpoint of impact dynamics.

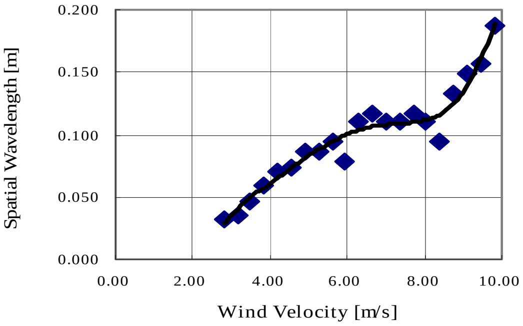

Fig. 6 The spatial wavelength of the wave observed in the array of 1000 polycarbonate rods as a function of wind velocity

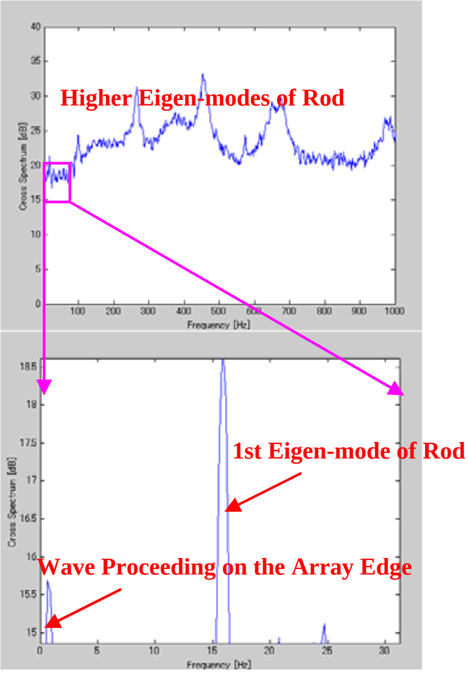

Fig. 7 Cross-spectrum analysis between the acceleration signal from the front-left rod and that from the back-left rod in the array of 1000 polycarbonate rods

References

[1] Kuroda, M., Moon, F. C., "Local Complexity and Global Nonlinear Modes in Large Arrays of Fluid-Elastic Oscillators," *CD-ROMs of ASME IMECE 2002*, Vol. 3 (IMECE2002-32752), pp. 1-11, 2002.

[2] M.A. Davies, F.C. Moon: Transition from soliton to chaotic motion during impact of a nonlinear elastic structure, *Chaos, Solitons & Fractals*, Vol. 4, Issue 2, (1994) 275-283.